Cancer Therapy: Preclinical

Clinical Cancer Research

Histone Deacetylase Inhibitor Enhances the Efficacy of MEK Inhibitor through NOXA-Mediated MCL1 Degradation in Triple-Negative and Inflammatory Breast Cancer

Angie M. Torres-Adorno[1,2], Jangsoon Lee[2], Takahiro Kogawa[2], Peter Ordentlich[3], Debu Tripathy[2], Bora Lim[2], and Naoto T. Ueno[2]

Abstract

Purpose: Inflammatory breast cancer (IBC), diagnosed clinically, and triple-negative breast cancer (TNBC), diagnosed by molecular receptor status, are the two most aggressive forms of breast cancer, and both lack effective targeted therapies. We previously demonstrated involvement of histone deacetylase (HDAC) inhibitor entinostat in regulating apoptosis in IBC and TNBC cells; here, we aimed to identify novel combination therapy candidates.

Experimental Design: Potential therapeutic targets were identified by mRNA expression profiling of TNBC and IBC cells treated with entinostat. Drug action and synergism were assessed by *in vitro* proliferation assays, tumor growth *in vivo*, and proteomic analyses. Gain/loss-of-expression studies were utilized to functionally validate the role of identified targets in sensitivity of TNBC and IBC cells to combination therapy.

Results: Entinostat induced activity of the oncogenic ERK pathway and expression of proapoptotic NOXA. These are known to stabilize and degrade, respectively, MCL1, an antiapoptotic Bcl-2 protein. In breast cancer patients, high-MCL1/low-NOXA tumor expression correlated significantly with poor survival outcomes. Combination treatment of entinostat with MEK inhibitor pimasertib reduced the growth of TNBC and IBC cells *in vitro* and inhibited tumor growth *in vivo*. The synergistic action of combination therapy was observed in TNBC and IBC cell lines in which NOXA expression was induced following entinostat treatment. The therapeutic activity depended on induction of mitochondrial cell death pathways initiated by NOXA-mediated MCL1 degradation.

Conclusions: Our preclinical findings provide a rationale for the clinical testing of combination HDAC and MEK pathway inhibition for TNBC and IBC that exhibit elevated baseline tumor MCL1 expression. *Clin Cancer Res; 23(16); 4780–92. ©2017 AACR.*

Introduction

Inflammatory breast cancer (IBC) and triple-negative breast cancer (TNBC) are the two most aggressive forms of breast cancers, representing 1%–5% and 10%–17% of all breast carcinomas, respectively (1, 2). Both are heterogeneous diseases and yet are often characterized by their strong metastatic potential and poor prognosis (3). TNBC, diagnosed molecularly in terms of negative estrogen receptor (ER), progesterone receptor (PgR), and HER2 status, has poorer prognosis compared with ER/PgR-positive and HER2-positive breast cancers (4). IBC, a clinical diagnosis, has worse prognosis across all molecular subtypes when compared with noninflammatory forms of breast cancer (non-IBC) cases (5). TNBC accounts for about 30% of IBCs molecular subtype, which is a significantly higher proportion when compared with non-IBCs (1, 6). There is speculation in the breast cancer field that this high percentage of TNBC may be the reason that IBC has been associated with a more aggressive clinical course and decreased overall and breast cancer–specific survival (7). Current standard of care is chemotherapy, with moderate efficacy. Lack of molecular and biological understanding of IBC and TNBC hampers the development of new targeted therapies that may lead to effective treatments. Therefore, there is an urgent and unmet need to define the biology of IBC and TNBC tumors, which could lead to an improved strategy to treat these aggressive breast cancers.

Epigenetic modulation in malignancies often silences genes that regulate proliferation and metastasis, thereby contributing to tumor aggressiveness. Histone deacetylases (HDAC) are critical regulators of gene expression; they do so through enzymatic removal of acetyl groups from histones that modify DNA access to the transcriptional machinery. Aberrant expression of HDACs, leading to tumorigenesis, is seen in multiple types of human cancers. In the last decade, multiple HDAC inhibitors have been developed as anticancer drugs and have shown antitumor action (8). Entinostat (formerly MS-275, Syndax Pharmaceuticals, Inc.), a selective class I HDAC inhibitor with low toxicity to normal cells, is a synthetic benzamide derivative that can reduce the

[1]UT Health Graduate School of Biomedical Sciences, The University of Texas MD Anderson Cancer Center, Houston, Texas. [2]Section of Translational Breast Cancer Research, Morgan Welch Inflammatory Breast Cancer Research Program and Clinic, Department of Breast Medical Oncology, The University of Texas MD Anderson Cancer Center, Houston, Texas. [3]Syndax Pharmaceuticals, Inc., Waltham, Massachusetts.

Note: Supplementary data for this article are available at Clinical Cancer Research Online (http://clincancerres.aacrjournals.org/).

Corresponding Authors: Naoto T. Ueno and Jangsoon Lee, The University of Texas MD Anderson Cancer Center, 1515 Holcombe Boulevard, Houston, TX 77030-4009. Phone: 713-792-2817; Fax: 713-794-4385; E-mail: nueno@mdanderson.org; Jangsoon Lee, jslee@mdanderson.org

doi: 10.1158/1078-0432.CCR-16-2622

Translational Relevance

The lack of molecular understanding of aggressive breast cancers, such as inflammatory breast cancer (IBC) and triple-negative breast cancer (TNBC), hampers the development of effective novel targeted therapies. In this study, we have identified a novel combination treatment of histone deacetylase (HDAC) type I and MEK inhibitors, entinostat and pimasertib, for the treatment of IBC and TNBC. Our *in vitro* and *in vivo* studies revealed significant synergistic antitumor activity of entinostat and pimasertib, via effective degradation of MCL1 through increased NOXA expression, leading to the induction of apoptosis. Indeed, we confirmed that in patients with aggressive breast cancer, high-MCL1/low-NOXA tumor expression correlated to poor survival outcomes compared with low-MCL1/high-NOXA expression. Our data provide a preclinical rationale to develop this novel combination of entinostat and pimasertib in the treatment of patients with TNBC and IBC, and validation of MCL1/NOXA modulation as a predictive biomarker of therapy.

proliferation of cancer cells and tumors xenografts in a variety of human cancers (9). Entinostat also displayed preliminary therapeutic efficacy in a randomized phase II clinical trials for ER-positive breast cancer patients (10). Although it is not known from available clinical trials whether entinostat can induce the expression of proapoptotic proteins in IBC and TNBC tumors, our recent preclinical study demonstrated entinostat-induced expression of the proapoptotic BIM protein in IBC and TNBC (11), suggesting the induction of apoptosis as a major mechanism of tumor suppression. We also identified increased transcription of NOXA (also called phorbol-12-myristate-13-acetate-induced protein 1, or PMAIP1), a member of the Bcl-2 family of apoptosis-regulating proteins, in 65% of TNBC and IBC cell lines following entinostat treatment.

The Bcl-2 family of proteins are critical modulators of apoptosis, acting immediately upstream of irreversible cellular damage, where antiapoptotic and proapoptotic family members control the release of apoptogenic factors from mitochondria (12). NOXA, a Bcl-2 homology domain 3 (BH3)-only proapoptotic protein, is epigenetically silenced by histone acetylation in cancer (13, 14). Independently, NOXA displays weak proapoptotic activity; however, it is a crucial modulator of cell death induction thought its ability to interact with the prosurvival Bcl-2 molecule MCL1 (induced myeloid leukemia cell differentiation protein 1). MCL1 is commonly amplified in TNBC and has been shown to be an adverse prognostic factor for survival (15). Degradation of MCL1 during cell death is uniquely associated with the formation of an MCL1/NOXA complex, while stabilization of MCL1 is associated with its ability to bind other BH3-only members (i.e., PUMA or BIM; refs. 16–18). Alternatively, MCL1 protein can be stabilized through the activation of the MAPK/extracellular signal-regulated kinase (ERK) signaling pathway, which promotes survival and drug resistance in cancer cells (19–21). As MCL1 is crucial to cancer cell survival, drugs that target the ERK pathway may have therapeutic value through their ability to reduce MCL1 expression.

ERK is an important therapeutic target in TNBC; high ERK expression correlates with shorter patient overall survival (22). While ERK inhibitors have not been effective in clinical testing, compounds that inhibit MEK (an upstream activator of ERK) including selumetinib (formerly AZD6244; refs. 23, 24), and the more potent compound pimasertib (formerly AS703026, EMD Serono, Inc.; refs. 25, 26) have displayed clinical activity in phase II trials for melanoma and ovarian cancer (27, 28). While the effectiveness of these compounds remains to be clinically established in breast cancer, we have previously shown their potential for preventing metastasis in preclinical xenograft models of TNBC (29). As such, we hypothesize that a combination therapy utilizing pimasertib (ERK inhibitor) and entinostat (HDAC inhibitor) would be effective due to parallel inhibitory effects on MCL1 protein levels in TNBC and IBC.

In the study presented here, we identified that high-MCL1/low-NOXA mRNA expression within primary breast tumors correlated with poor survival outcomes in breast cancer patients. Using *in vitro* and *in vivo* preclinical models, we demonstrate that NOXA and MCL1 play important roles in the regulation of IBC and TNBC cells sensitivity to entinostat and pimasertib combination treatment. Collectively, our data provides the rationale for developing a targeted MEK/HDAC combination therapy for patients with TNBC and IBC that have high baseline MCL1 expression.

Materials and Methods

Detailed information regarding co-immunoprecipitation, TUNEL staining, and chromatin immunoprecipitation (ChIP) is included in electronic supplementary material. Detailed information about *in vitro* cell proliferation assay, apoptosis analysis, soft agar assay, transfections, immunoblotting analysis, and IHC is provided in our previous publication that describes the effect and mechanism of action of entinostat (11).

Breast cancer patient tumor expression analysis

We analyzed the World IBC Consortium dataset that contains Affymetrix GeneChip (HGU133 series) RNA hybridization profiles of 389 breast cancer patient samples, which include 137 IBC cases and 105 TNBC cases, as previously described (30). Briefly, the IBC cases included locally advanced [American Joint Committee on Cancer (AJCC) stage III] and metastatic (AJCC stage IV) cases. The non-IBC cases included both early-stage disease (AJCC stages I and II) and advanced-stage disease (locally advanced, AJCC stage III; and metastatic, AJCC stage IV). Information on data processing, normalization, and analyses has been previously reported (31). Regression models were used to delineate changes in *NOXA/PMAIP1* (204286_s_at) and *MCL1* (214056_at) gene expression. *P* values, corrected for multiple comparisons, were considered significant only if the false discovery rate was smaller than 0.25.

Cell lines

Human breast cancer cell lines BT-549, SUM185PE, MDA-MB-157, MDA-MB-453, MDA-MB-231, HCC70, MDA-MB-468, MDA-MB-436, HCC1806, HCC1937, and Hs578T were purchased in 2011 from ATCC; SUM149PT, SUM159PT, and SUM190PT cells in 2011 from Asterand Bioscience, Inc.; and HCC3153 in 2013 from UT Southwestern Medical Center (Dallas, TX). KPL-4 cells were a kind gift in 2008 from Dr. Junichi Kurebayashi (Kawasaki Medical School, Kawasaki, Japan), and IBC-3 cells from Dr. Wendy Woodward (The University of Texas MD Anderson Cancer Center, Houston, TX). HCC1806,

MDA-MB-231, MDA-MB-468, MDA-MB-436, MDA-MB-157, MDA-MB-453, Hs578T, HCC70, and KPL-4 cells were maintained in DMEM/F12 medium (Gibco) supplemented with FBS (10%) and penicillin–streptomycin (100 U/mL). SUM149PT, SUM190PT, SUM185PE, SUM159PT, and IBC-3 cells were maintained in F12 medium (Gibco) supplemented with FBS (5%), penicillin–streptomycin (100 U/mL), insulin (5 μg/mL), and hydrocortisone (1 μg/mL). BT-549, HCC1937, and HCC3153 cells were maintained in RPMI1640 medium (Gibco) supplemented with FBS (10%) and penicillin–streptomycin (100 U/mL). SUM190PT, SUM149PT, IBC-3, and KPL-4 are IBC cell lines (32, 33). All cell lines were passaged for up to 20 times after thawing. Details about molecular receptor status and TNBC subtype classification can be found in Supplementary Table S1 (34). All used cell lines were authenticated by genotyping through MD Anderson Cancer Center's Characterized Cell Line Core Facility, and routinely tested for mycoplasma contamination using MycoAlert (Lonza).

Reagents and antibodies

Entinostat (SNDX-275) was provided by Syndax Pharmaceuticals, Inc. Pimasertib (AS703026) was provided by EMD Serono, Inc. We obtained anti-NOXA (EMD Millipore), anti-MCL1 (R&D Systems or Thermo Fisher Scientific), anti-PUMA, anti-BIM, anti-BAK, anti-BAX, anti-cleaved caspase-3, anti-cleaved caspase-9, and anti-Ki67 (Cell Signaling Technology), anti-α-tubulin (clone B-5-1-2; Sigma-Aldrich), and anti-horseradish peroxidase–conjugated antibodies (Thermo Scientific). The following siRNAs targeting NOXA were purchased from Sigma-Aldrich and used for depletion of NOXA: SASI_Hs01_00136187, SASI_Hs01_00136188, SASI_Hs01_00136189, and SASI_Hs01_00136192. Knockdown efficacy of pooled siRNAs was tested by immunoblotting. Scrambled siRNA was purchased from Thermo Fisher Scientific (ON-TARGETplus nontargeting control pool, catalog number D-001810). The following expression vectors were purchased from GeneCopoeia: OmicsLink pReveiver-M77 expression clone NOXA (EX-I0491-M77), MCL1 (EX-G0192-M77), and Control (EX-EGFP-M77).

Quantitative real-time PCR

Total RNA was purified using the PureLink RNA Mini Kit (Invitrogen), and real-time qRT-PCR was performed using the iScript One-Step RT-PCR Kit with SYBR Green (Bio-Rad) according to the manufacturer's instructions, after treatment with entinostat (1 μmol/L). Equal amounts of total RNA (15 ng for each sample) were mixed, and target genes were amplified with a specific primer set using the CFX96Touch Real-Time PCR Detection System (Bio-Rad). The following primers (Sigma-Aldrich) were used for detection of NOXA: 5′-CCAGCAGAGCTGGAAGTCGAGTG-′3 (forward), and 5′-TGCAGTCAGGTTCCTGAGCAGAAG-′3 (reverse). 7SL scRNA (NR_002715.1) levels were used as an endogenous control; the following primers were used: 5′-ATCGGGTGTCCGCACTAAGTT-′3 (forward), and 5′-CAGCACGGGAGTTTTGACCT-′3 (reverse). The real-time PCR data were analyzed by comparative threshold cycle method using the iCycler CFX96 analyzer software (Bio-Rad).

In vivo xenograft animal models

Animal studies were approved by the Institutional Animal Care and Use Committee and MD Anderson Animal Care and Use Committee. Female athymic homozygous *nu/nu* mice, age 4–6 weeks old, were purchased from MD Anderson's Department of Experimental Radiation Oncology for the SUM190PT, SUM149PT, and MDA-MB-231 xenograft experiments. Mice were

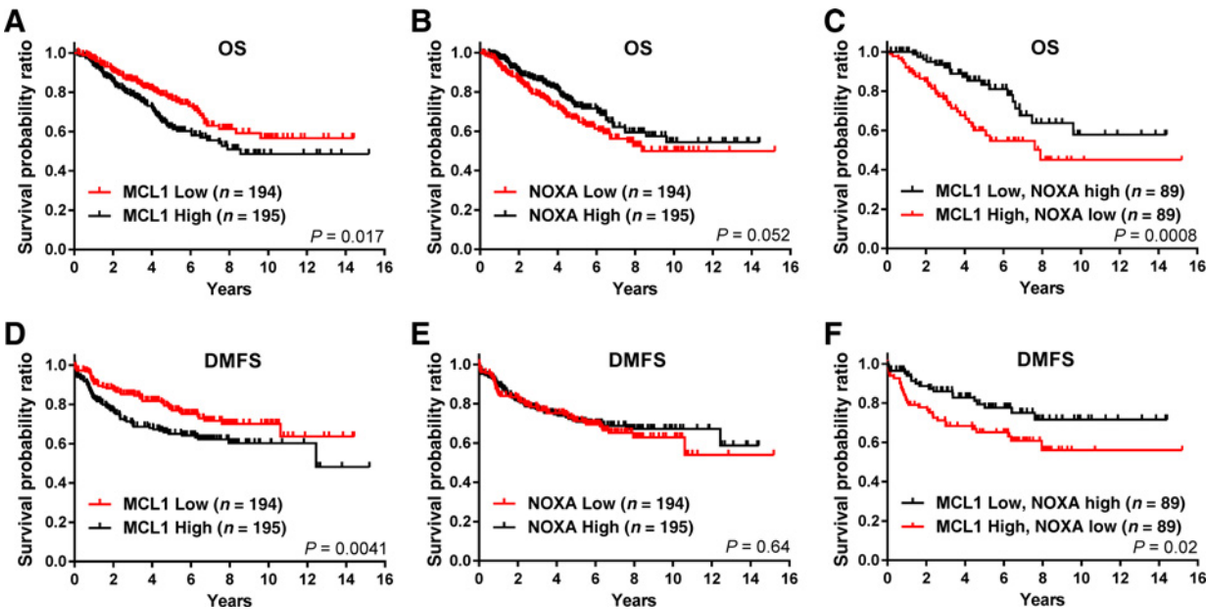

Figure 1.

High MCL1/low NOXA coexpression is associated with poor outcome in breast cancer patients. Kaplan–Meier survival curves for overall survival (OS) and distant metastasis-free survival (DMFS) of breast cancer patients from the IBC World Consortium dataset, correlated to *NOXA* and *MCL1* tumor mRNA levels. The log-rank test was used to compare survival curves for high and low MCL1 (**A**, **D**), high and low NOXA (**B**, **E**), and high or low MCL1 in correlation with low or high NOXA (**C**, **F**). The initial numbers of patients at risk in each group are indicated in the key.

housed under pathogen-free conditions and treated in accordance with NIH guidelines. To establish breast cancer xenografts, SUM190PT (2×10^6 cells/100 μL), SUM149PT (5×10^6 cells/100 μL), or MDA-MB-231 (5×10^6 cells/100 μL) cell suspensions were injected into one site in the abdominal mammary fat pad of each mouse. We observed 100% tumor incidence for all three cell lines. Drug treatments via daily oral gavage started when the tumors were approximately 100–150 mm^3. We used 0.5% (w/v) methyl cellulose 400 solution (Wako Pure Chemical Industries, Ltd.) plus 0.25% Tween 20 as drugs vehicle. Tumor volume [$V = 0.5 \times (L \times W^2)$] and body weight were measured twice weekly. Drug treatment continued for 28 days (SUM190PT), 56 days (SUM149PT), or 42 days (MDA-MB-231), and then mice were euthanized. Tumor samples were collected at biopsy, and sections preserved both by freezing and paraffin block embedding for downstream applications.

Statistical analysis

For experimental outcomes, descriptive statistics (mean and SEM) were summarized for each group. An ANOVA model was used to compare the mean outcome values among the tested groups. Statistical analyses were performed using an unpaired *t*-test with Prism version 5 (GraphPad Software). *P* values of <0.05 were considered statistically significant.

Results

NOXA and MCL1 expression are molecularly and clinically relevant to entinostat and pimasertib treatment in IBC and TNBC

In our previous study, we observed entinostat-induced expression of the proapoptotic protein BIM in TNBC and IBC cell lines, suggesting the induction of apoptosis as a major mechanism of tumor suppression (11). To identify apoptosis-related molecular changes induced by entinostat in TNBC and IBC cells following treatment, we performed a quantitative PCR array with 28 apoptosis-related probes on two established cell lines: SUM190PT (IBC), and SUM149PT (IBC-TNBC), chosen because of their IBC and TNBC status. We found that *NOXA*/*PMAIP1* was among the top upregulated apoptosis-related mRNAs after 48 hours of entinostat treatment on both cell lines (Supplementary Table S2), consistent with previous observations in acute myeloid leukemia (35). Because NOXA promotes intrinsic apoptosis through proteasomal degradation of the antiapoptotic protein MCL1, while the ERK pathway is known to support MCL1's stabilization, we next analyzed the effect of entinostat on the phosphorylation/activation of ERK (p-ERK) in IBC (IBC3, KPL-4, SUM149PT, and SUM190PT) and non-IBC (BT-474, MDA-MD-231, MDA-MB-468, and SKBR3) cell lines. After 48 hours of treatment, entinostat induced p-ERK expression in IBC (3 of 4) and TNBC (MDA-MB-468) while no inducing effect was observed on another major cancer-related pathway, AKT, among the tested cell lines (Supplementary Fig. S1). These results suggest p-ERK could act as a stabilizer for MCL1 in IBC and TNBC, representing a potential target that could enhance apoptosis in combination with entinostat treatment.

On the basis of this observation, we pursued further studies addressing how NOXA/MCL1 expression may contribute to the therapeutic efficacy of combining entinostat and an ERK pathway inhibitor in IBC and TNBC. We first determined the clinical relevance of NOXA and MCL1 expression levels to breast cancer patient outcome. We analyzed a previously published cDNA microarray dataset of breast cancer patient samples, which contains IBC (35%) and non-IBC (65%; 27% TNBC) cases (30). Kaplan–Meier survival analysis revealed that low MCL1 mRNA expression levels within patient tumors significantly correlated with longer patient overall survival (OS) and distant metastasis-free survival (DMFS) than high MCL1 mRNA levels ($P = 0.017$ and 0.0041, respectively; Fig. 1A and D). Conversely, high NOXA expression was associated with longer OS (a nearly significant difference, $P = 0.052$), but not DMFS (nonsignificant, $P = 0.64$) in this cohort (Fig. 1B and E). When stratified by both MCL1 and NOXA tumor expression, significantly longer OS and DMFS were seen in patients with low MCL1/high NOXA expression than in patients with high MCL1/low NOXA expression ($P = 0.0008$ and 0.02, respectively; Fig. 1C and F).

Next, we investigated NOXA and MCL1 *in vitro*. Using quantitative real-time PCR analysis, and chromatin immunoprecipitation (ChIP), we confirmed increased *NOXA* mRNA expression associated with *NOXA* gene promoter acetylation levels following entinostat treatment (1 μmol/L) in SUM190PT and, to a lesser degree, SUM149PT cells, compared with the untreated control (Supplementary Fig. S2). To further confirm this finding, we screened other IBC (KPL-4 and IBC-3) and TNBC (SUM159PT,

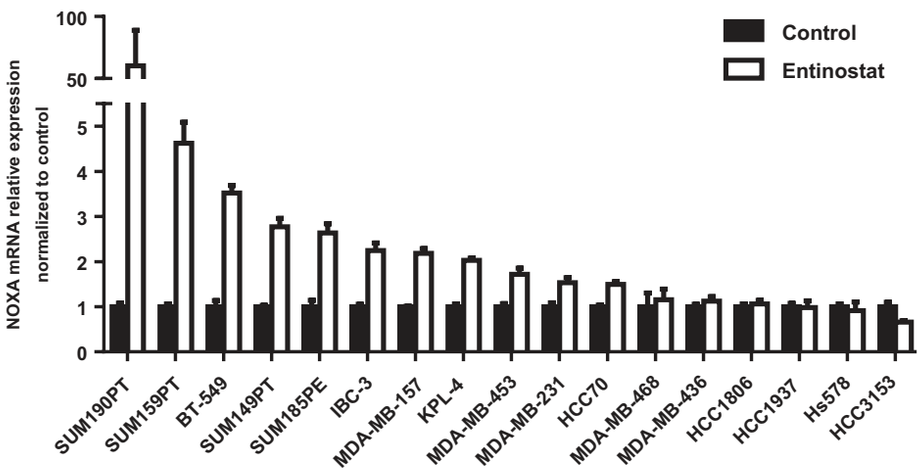

Figure 2.
Entinostat treatment selectively increases expression of *NOXA* mRNA in TNBC and IBC cell lines. *NOXA* mRNA levels were analyzed in multiple TNBC and IBC cell lines using quantitative real-time PCR after 48 hours of treatment with entinostat (1 μmol/L), compared with the untreated control. Data were pooled from three independent experiments.

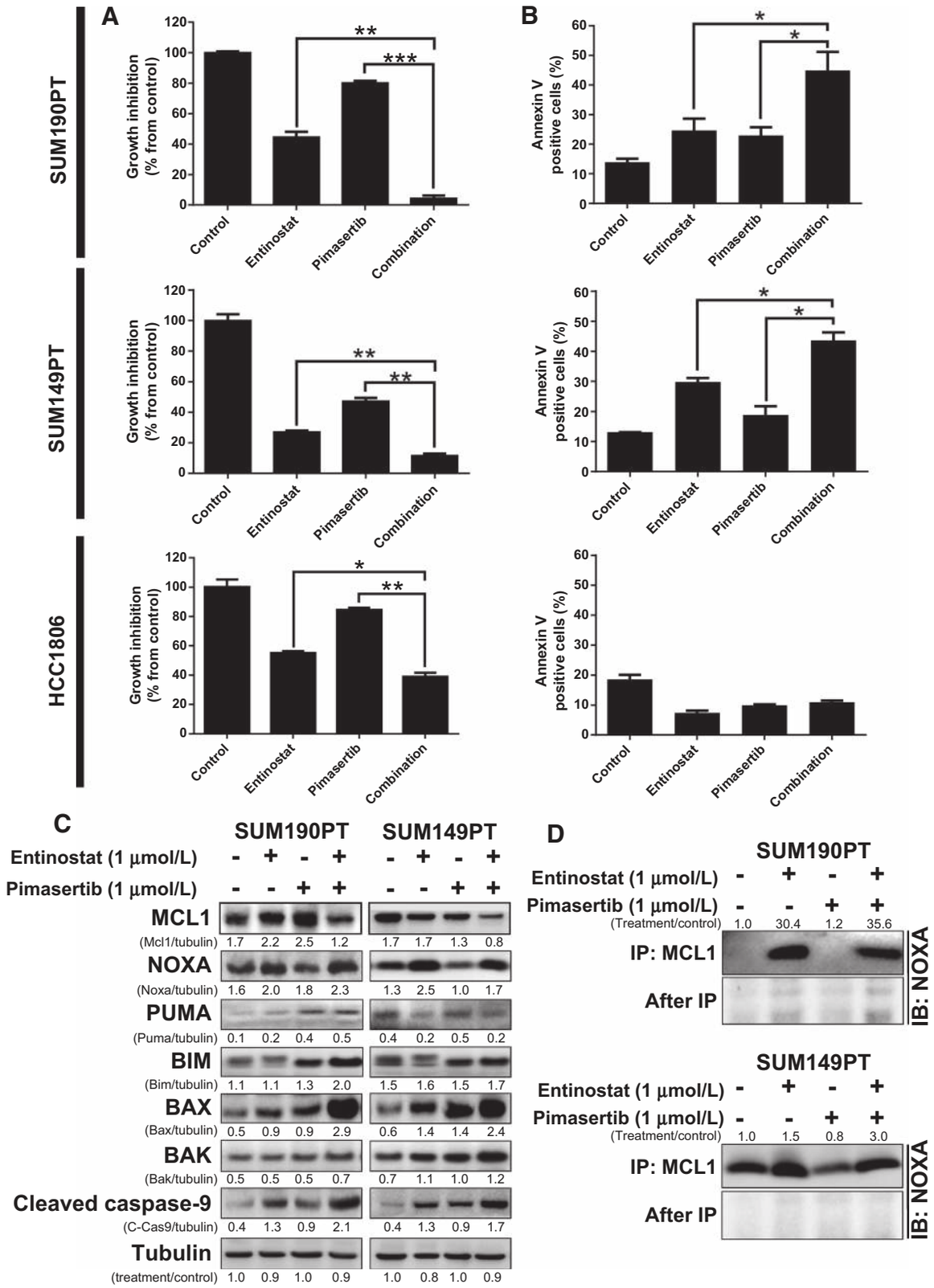

BT-549, SUM185PE, MDA-MB-157, MDA-MB-453, MDA-MB-231, HCC70, MDA-MB-468, MDA-MB-436, HCC1806, HCC1937, HCC3153, and Hs578T) cell lines (Fig. 2; Supplementary Table S1). Compared with untreated cell lines, *NOXA* mRNA was induced by entinostat treatment in 65% (11 of 17) of the IBC and TNBC cell lines tested. Immunoblotting analysis was performed on all cell lines to identify relationships between protein expression levels of NOXA and MCL1 after entinostat treatment (data shown for 12 cell lines, Supplementary Fig. S3). NOXA protein expression did not positively correlate with increased *NOXA* mRNA expression levels, possibly due to the short protein half-life of NOXA through proteasome-dependent degradation (36). We also identified detectable levels of MCL1 protein expression in 80% of cell lines, as defined by MCL1/tubulin pixel density $\geq$ 0.4 (the average MCL1 pixel density among all cell lines), and observed induction of MCL1 protein expression in multiple cell lines following entinostat treatment. Together with our preliminary data demonstrating that entinostat mediated p-ERK expression (Supplementary Fig. S1), the changes in protein levels of MCL1 suggest the stabilization of MCL1 through p-ERK pathway activation in TNBC and IBC cells.

Entinostat and pimasertib combination therapy synergize to inhibit the growth of aggressive breast cancer cells that overexpress NOXA after entinostat treatment

As a monotherapy for TNBC and IBC, the efficacy of entinostat may be hindered due to the induction of MCL1 through p-ERK activation. Thus, we hypothesized that addition of the MEK inhibitor pimasertib may potentiate cellular cytotoxicity of entinostat by simultaneously blocking ERK activation. Synergistic killing by the combination therapy was observed in 12 of 17 IBC and TNBC cell lines tested (representative data shown for three cell lines, Fig. 3A), with response predominantly correlated to each cell line's level of *NOXA* mRNA induction after entinostat treatment [representative data for combination index (CI) shown for eight cell lines, Supplementary Fig. S4]. Sixty percent of cell lines responding to combination therapy had high basal MCL1 protein levels (MCL1/tubulin pixel density $\geq$ average, 0.4; Supplementary Fig. S3), while the other 40% of responding cell lines displayed synergistic cell killing despite low MCL1 expression, which may be associated with the induced levels of NOXA, as observed in Fig. 2. Therefore, the effectiveness of combination treatment was correlated to *NOXA*-mRNA–inducible cell lines, potentially inducing apoptosis by enhanced targeting of MCL1, providing a mechanism that could circumvent the problems associated with monotherapy.

To determine cell death induction levels after treatment, we next analyzed the effect of entinostat and pimasertib on apoptosis after dose response experiments of clinically achievable ($\leq$1 μmol/L) doses. The SUM190PT and SUM149PT cell lines were selected for further analysis based on their TNBC and/or IBC status, as well as their significant induction of NOXA-mRNA following entinostat treatment. The HCC1806 TNBC cell line was selected as a negative control based on its lack of entinostat-mediated NOXA-mRNA induction and apparent resistance to treatment. As shown in Fig. 3B, single entinostat or pimasertib treatment induced apoptosis by 10% and 9%, respectively, in SUM190PT cells and by 16% and 6% in SUM149PT cells, compared with the control (untreated cells). However, combination treatment significantly increased the proportion of apoptotic cells by 30% in SUM190PT and SUM149PT cells compared with the control. The TNBC cell line HCC1806 did not respond to single or combination treatment, which correlates to its inability to express NOXA following entinostat treatment (Fig. 2). Collectively, these data suggest that the combination of entinostat and pimasertib is most effective in TNBC and IBC cell lines in which NOXA can be induced.

As the efficacy of the combination therapy correlated with the induction of proapoptotic NOXA, we next assessed the broader spectrum of proteins involved during apoptosis. We initially assessed the effect of single and combination therapy on the expression of downstream pathway members BIM, BAK, BAX, PUMA, and caspase-9 (Fig. 3C). After 48 hours of treatment, we found that the antiapoptotic MCL1 protein was reduced, while the NOXA-regulated, proapoptotic BCL-2 proteins BIM, BAX, and BAK were elevated in two IBC cell lines. As expected, we detected increased levels of cleaved caspase-9, which indicates the induction of apoptosis in these cell lines. As a negative control, we did not observe alterations in MCL1, NOXA, or cleaved caspase-9 in the therapeutically insensitive HCC1806 cells (Supplementary Fig. S5A), consistent with this cell line's observed lack of apoptosis induction following combination treatment (Fig. 3B). PUMA expression was not consistently altered after single or combination treatments, suggesting that it may not play a main role in MCL1 degradation. These data suggest that NOXA-based regulation of apoptosis may be responsible for therapeutic efficacy in TNBC and IBC.

Because NOXA can bind to and enhance the degradation of MCL1 protein (18), and we had observed induction of NOXA expression and increased apoptosis in cell lines sensitive to combination therapy, we hypothesized that NOXA-MCL1 binding may contribute to cell death with our therapy. To confirm whether NOXA bound MCL1 in our system, we performed an MCL1 immunoprecipitation assay on cell lines following treatment. Following MCL1 precipitation, we were able to detect elevated NOXA protein by immunoblotting analysis in two cell lines treated with both entinostat and pimasertib (Fig. 3D). These results suggest that our combination therapy leads to enhanced apoptosis in TNBC and IBC cells by reducing MCL1 expression potentially through NOXA-mediated degradation of MCL1.

Figure 3.

Entinostat and pimasertib combination treatment enhanced cell death in IBC and TNBC cell lines that overexpressed NOXA after entinostat treatment. SUM190PT, SUM149PT, and HCC1806 cells were treated with clinically achievable ($\leq$1 μmol/L) doses, representative data shown for entinostat (1 μmol/L) and pimasertib (1 μmol/L) for 48–72 hours. The IC_{50} values of entinostat were determined for SUM190PT, SUM149PT, and HCC1806 cell lines to be 0.6 μmol/L, 0.3 μmol/L, and 0.9 μmol/L, respectively; the IC_{50} values of pimasertib were 1.9 μmol/L, 0.6 μmol/L, and 2.5 μmol/L, respectively. Cell proliferation and apoptosis were measured by SRB staining (**A**) and Annexin V-PE staining (**B**), respectively. Data were pooled from three independent experiments and presented as mean ± SEM. *, $P < 0.05$; **, $P < 0.001$; ***, $P < 0.0001$. MCL1, NOXA, PUMA, and mitochondrial apoptosis-related proteins BIM, BAX, BAK, and cleaved caspase-9 were examined through immunoblotting analysis (**C**). **D,** NOXA/MCL1 binding on SUM190PT and SUM149PT cells was determined after entinostat (1 μmol/L) and pimasertib (1 μmol/L) individual and combination treatment by immunoprecipitation (IP) using anti-MCL1 antibody and immunoblotting with anti-NOXA antibody. After immunoprecipitation, samples were also blotted with NOXA antibody as an immunoprecipitation control. Pixel density of proteins was quantified for each condition, and the ratios of protein/tubulin or treatment/control are shown next to the blots; tubulin expression was used as a protein loading control.

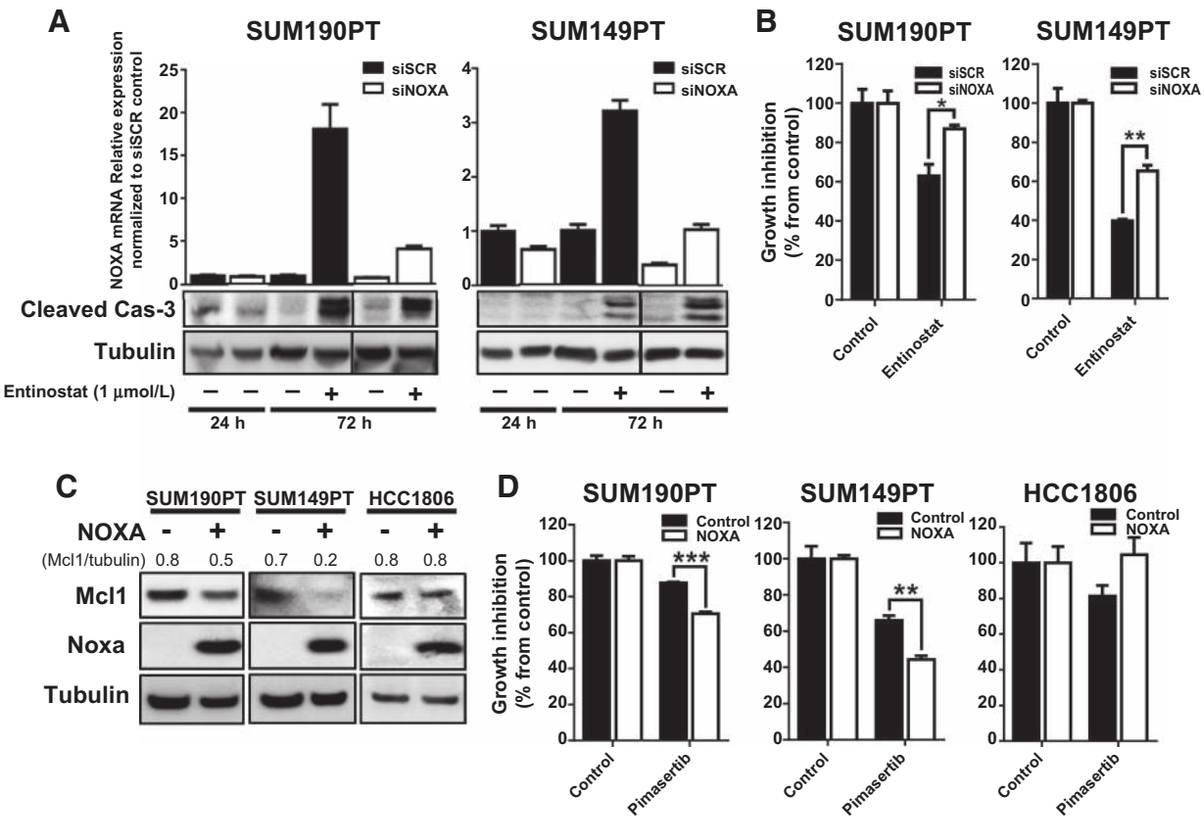

Figure 4.

NOXA expression plays an important role in the regulation of sensitization of TNBC and IBC cells to treatment. SUM190PT and SUM149PT cells were transfected with NOXA (siNOXA) or Scrambled (siSCR) siRNA through electroporation. Knockdown of *NOXA* mRNA and induction of apoptosis as measured by cleaved caspase-3 after siRNA inhibition were confirmed by quantitative RT-PCR and immunoblotting analysis (**A**), respectively, after entinostat treatment for 24 and 72 hours. Cell proliferation after siRNA and entinostat treatment was measured by SRB staining after 72 hours (**B**). SUM190PT, SUM149PT, and HCC1806 cells were transfected with either a NOXA-expressing vector or empty control vector by electroporation. Expression of NOXA, as well as MCL1, was analyzed by immunoblotting analysis 72 hours after transfection (**C**). Pixel density of MCL1 was quantified for each condition, and the ratios of MCL1/tubulin are shown above the blots; tubulin expression was used as a protein loading control. Proliferation of cells with NOXA overexpression in response to treatment with pimasertib (2.5 μmol/L) was determined by SRB staining after 72 hours (**D**). Data were pooled from three independent experiments and presented as mean ± SEM. *, $P < 0.05$; **, $P < 0.005$; ***, $P < 0.0001$.

NOXA and MCL1 play important roles in regulation of sensitization of IBC and TNBC cells to entinostat and pimasertib treatment

To determine whether NOXA is a critical component in defining the therapeutic efficacy of entinostat and pimasertib, we functionally silenced *NOXA* mRNA expression and assessed the response of SUM190PT and SUM149PT cells to treatment (Fig. 4A). When treated with entinostat, NOXA-silenced SUM190PT and SUM149PT cells did not display altered activation of caspase-3, however the loss of NOXA expression hindered the cytotoxic effects of entinostat compared with scrambled siRNA control ($P < 0.05$, and $P < 0.005$, respectively; Fig. 4A and B). The unaltered induction of cleaved caspase-3 upon siNOXA inhibition is probably due to the high levels of *NOXA* mRNA that are still induced after entinostat treatment of siNOXA-transfected SUM190PT and SUM149PT cells (5- and 3-fold increase, Fig. 4A), permitting apoptosis. These results suggest a role for NOXA in enabling cytotoxicity after entinostat treatment.

In a reverse-complementary approach, we assessed whether transient overexpression of NOXA could modulate cells' response in combination with pimasertib in the treatment-sensitive SUM190PT and SUM149PT cells, or the treatment-resistant HCC1806 cells, which lack entinostat-mediated NOXA mRNA induction (Fig. 4C). Following overexpression of NOXA and pimasertib treatment, SUM190PT and SUM149PT cells had significant inhibition of cell proliferation compared with untreated cells ($P < 0.0001$, and $P < 0.005$, respectively; Fig. 4D), further supporting the significance of NOXA mediating MCL1 degradation and enhancing pimasertib treatment. In contrast, HCC1806 cells had increased resistance to pimasertib treatment after NOXA overexpression. These findings suggest that the HCC1806-resistant cell line could have an alternative mechanism by which it is able to override NOXA activity, possibly due to expression of other antiapoptotic proteins, or activation of cell survival pathways, avoiding NOXA-mediated apoptosis.

As we have demonstrated that NOXA can affect overall protein levels of MCL1 leading to altered drug sensitivity in IBC and TNBC

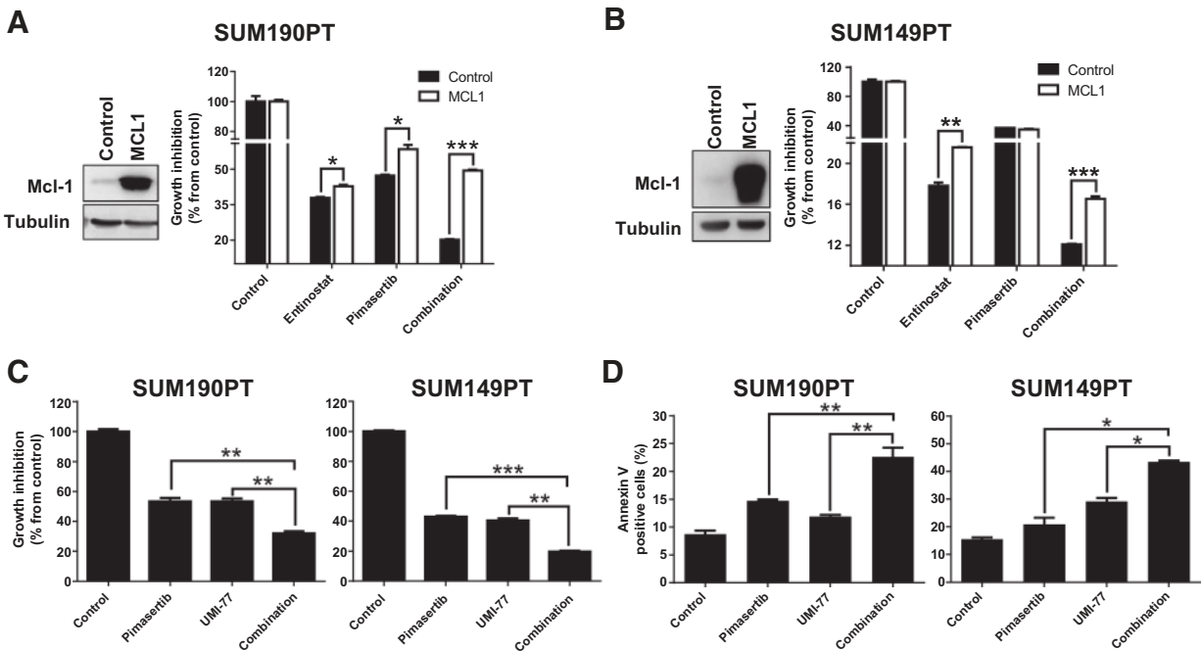

Figure 5.

MCL1 protein expression and activity have a significant role in the sensitivity of TNBC and IBC cells to pimasertib and entinostat combination treatment. SUM190PT and SUM149PT cells were transfected with either MCL1-expressing or empty control vectors by electroporation (**A**, **B**). Induced expression of MCL1 protein was confirmed by immunoblotting analysis. The ability of MCL1 overexpression to induce cell proliferation after entinostat (5 μmol/L) and pimasertib (5 μmol/L) single and combination treatments was measured by SRB staining after 72 hours. Cell proliferation (**C**) and apoptosis (**D**) were determined by SRB staining and Annexin V-PE staining, respectively, in SUM190PT and SUM149PT cells after inhibition of MCL1 by the small molecule inhibitor UMI-77 (0.3 μmol/L and 5 μmol/L, respectively) in combination with pimasertib (1 μmol/L). Data were pooled from three independent experiments and presented as mean ± SEM. Tubulin expression was used as a protein loading control. *, $P < 0.05$; **, $P < 0.001$; ***, $P < 0.0001$.

cells, we next assessed whether alteration of MCL1 could similarly modulate the therapeutic action of our rationalized combination treatment. Following transient MCL1 expression, entinostat and pimasertib single and combination treatments were tested in SUM190PT and SUM149PT cells (Fig. 5A and B). Overexpression of MCL1 significantly reversed the sensitivity of SUM190PT and SUM149PT cells to entinostat single ($P < 0.05$) and combination treatments ($P < 0.0001$). Conversely, when we treated SUM190PT and SUM149PT cells with a highly selective MCL1 inhibitor, UMI-77, in combination with pimasertib, we observed synergistic growth inhibition (CI values < 0.6 and 0.9, respectively; data not shown), accompanied by a significant induction of apoptosis compared with untreated control cells ($P < 0.05$; Fig. 5C and D). These data indicate that MCL1 is critical for the resistance of IBC and TNBC cells to treatment, and suggests a synergistic antiproliferative combination of pimasertib with inhibitors of MCL1 expression, such as through entinostat-mediated NOXA degradation of MCL1.

Entinostat and pimasertib combination treatment suppresses tumorigenic potential *in vitro* and *in vivo* tumor growth in xenograft models of aggressive breast cancer

Prior to the *in vivo* drug testing, we first assessed whether the combination of entinostat and pimasertib could affect the ability of TNBC and IBC cells to form anchorage-independent tumor spheroids *in vitro*. Preliminary studies indicated that the IC_{50} doses for both drugs were too toxic in this experimental setting to allow any colony growth (data not shown). Therefore, we selected lower doses than the IC_{50} for both entinostat and pimasertib. Combination treatment significantly reduced the number of colonies formed by SUM190PT and SUM149PT cells compared with single-drug treatments ($P < 0.05$; Fig. 6A), whereas in the treatment-resistant HCC1806 cells entinostat did not affected tumorigenicity, and pimasertib and combination treatment only mildly inhibited colony formation (Supplementary Fig. S5B).

After confirming reduced cell proliferation and anchorage-independent growth following entinostat and pimasertib combination treatment *in vitro*, we next determined whether these two drugs could inhibit tumor growth in preclinical xenograft animal models of TNBC and IBC. Mice ($n = 10$ to 12 per group) were treated with optimized doses of entinostat (20 mg/kg/day for SUM190PT, 5 mg/kg/day for SUM149PT), pimasertib (30 mg/kg/day for SUM190PT, 0.5 mg/kg/day for SUM149PT), or a combination of both drugs. When compared with mice treated with vehicle control, combination treatment mice displayed a significant reduction in tumor growth rate by 79% ($P < 0.0001$) and 65% ($P < 0.001$) in SUM190PT and SUM149PT cells, respectively (Fig. 6B). Of importance, while high-dose single treatment of entinostat (20 mg/kg) or pimasertib (30 mg/kg) significantly inhibited tumor growth (Fig. 6B; Supplementary Fig. S6A), at lower doses the combination treatment out performed single treatment in SUM149PT (Fig. 6B) and MDA-MB-231 xenografts (Supplementary Fig. S6B). Mice tolerated all treatments with no significant change in body weight noted (data not included).

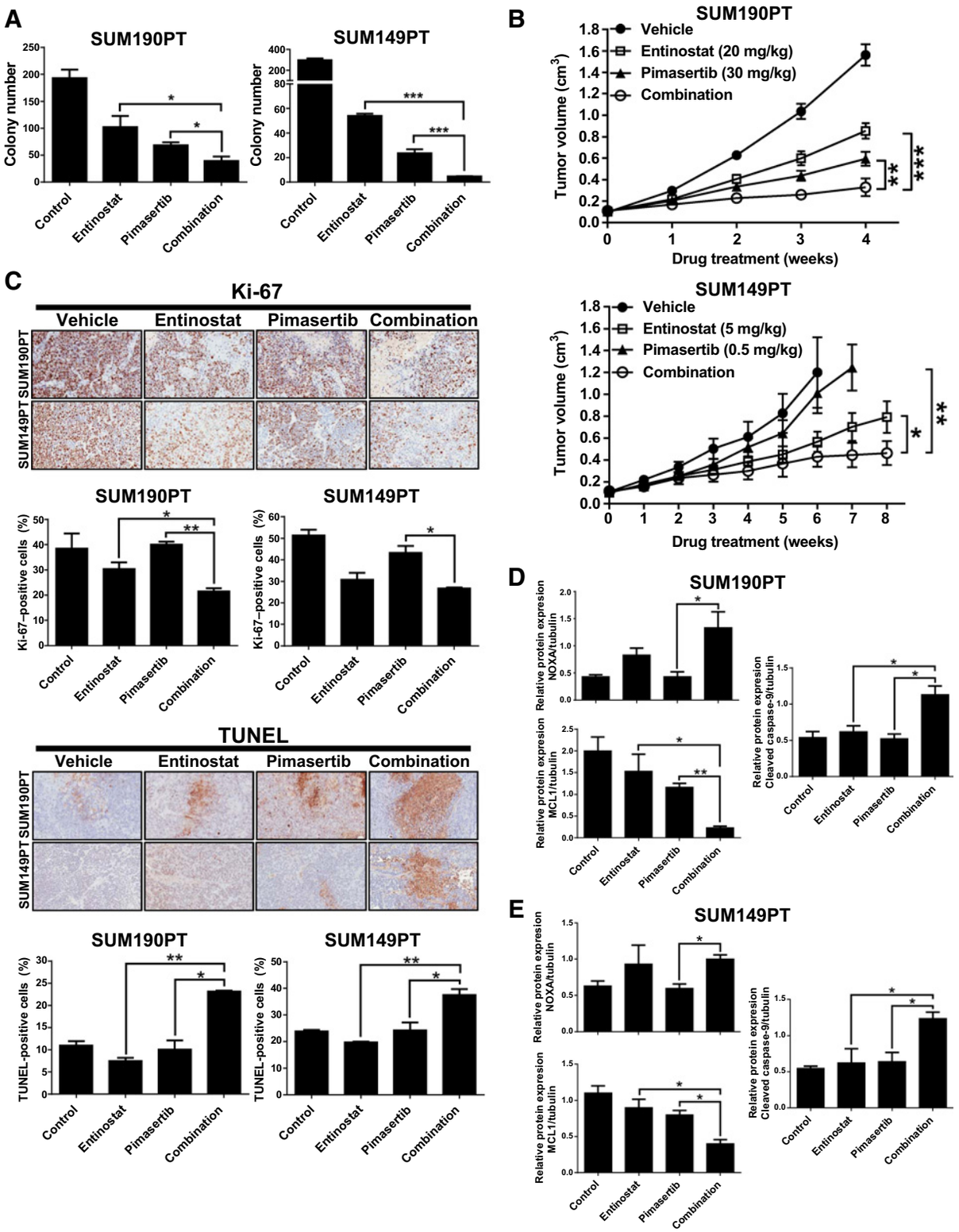

Immunostaining for markers of proliferation and cell death in SUM190PT, SUM149PT, and MDA-MB-231 primary tumors identified, as expected, a reduction of Ki67 positivity and an increase in TUNEL or cleaved caspase-3 staining in tumors receiving combination treatment (Fig. 6C; Supplementary Fig. S6B). Finally, after entinostat and pimasertib combination treatment, protein lysate expression of tumor samples from SUM190PT and SUM149PT xenograft models revealed higher protein expression of NOXA and its downstream marker of mitochondrial cell death, cleaved caspase-9, together with decreased expression of MCL1 (average protein expression quantified relative to tubulin loading control, $n = 5$ tumors per treatment group; Fig. 6D and E). Together, these results suggest increased apoptosis consistent with TUNEL staining following entinostat and pimasertib combination treatment through mediation of NOXA expression and subsequent degradation of MCL1 enhanced by pimasertib in TNBC and IBC.

Discussion

Our study has revealed that combination of entinostat and pimasertib synergistically act to reduce tumorigenic potential, proliferation, and *in vivo* growth of tumor using preclinical models of TNBC and IBC. The effectiveness of this treatment was significantly associated to the ability of tumors to induce *NOXA* mRNA expression following entinostat treatment, leading to enhanced degradation of the antiapoptotic protein MCL1 in IBC and TNBC. Furthermore, in our retrospective genomic analyses on an extensive clinical cohort of breast cancer patients, we were able to associate high-MCL1/low-NOXA tumor expression in breast tumors with worse OS and DMFS outcomes when compared with low-MCL1/high-NOXA–expressing tumors, which supports the translational potential for targeting these molecules in the clinical setting.

Several studies have demonstrated that entinostat induces apoptosis by expression of death receptor TNF-related apoptosis-inducing ligand (TRAIL) and transcriptional upregulation of proapoptotic Bcl-2 proteins BIM and NOXA in acute myeloid leukemia (35) and in HER2-overexpressing breast cancers (11), supporting chemosensitization (37). Here, we identified selective induction of *NOXA* mRNA expression after entinostat treatment in a subset of IBC and TNBC cell lines, which often correlated with increased protein expression of MCL1 as well as p-ERK, a known stabilizer of MCL1. Thus, our data suggest that besides the induction of NOXA after single entinostat treatment, additional p-ERK induction could play a role in the stabilization of antiapoptotic MCL1, supporting our strategy of testing an ERK pathway inhibitor, pimasertib, as a synergistic partner.

The interaction between MCL1 and NOXA contributing to apoptosis has been previously demonstrated, whereby MCL1 is recruited from the cytosol into the mitochondria by NOXA promoting BIM release from MCL1 sequestration, which initiates MCL1 phosphorylation and subsequent ubiquitination triggering proteasome-mediated degradation (17, 38). Here, we demonstrate that NOXA bound to MCL1 leading to its degradation following entinostat and pimasertib treatment. This was associated with activation of mitochondrial/proteasome-mediated apoptosis in SUM190PT and SUM149PT cell lines as measured through BIM, BAX, BAK, and caspase-3 and -9 cleavage *in vitro* and *in vivo*, whereas single or combination treatments failed to reduce tumorigenic potential and induce apoptosis in the treatment-resistant HCC1806 cells, which lack entinostat-mediated NOXA mRNA induction. We suggest that the minimal treatment effects inducing apoptosis on HCC1806 cells may be attributed to entinostat ability to inhibit cell proliferation by inducing p21-mediated G_1 cell-cycle arrest following low doses of entinostat treatment, as reported by others (39). Therefore, the clinically relevant entinostat doses tested in our study may not be effective at inducing apoptosis in the HCC1806 cell line. Further investigation is necessary to fully understand the potential mechanisms of inducing treatment resistance.

We recognize that there are slightly different treatment sensitivity levels observed between the SUM190PT and SUM149PT cell lines, which may be due to diverse NOXA/MCL1–binding abilities, NOXA mRNA induction levels, or SUM190PT HER2 positivity possibly affecting NOXA expression via TP53. There is evidence that HER2 signaling negatively regulates the function of TP53, a known positive regulator of NOXA expression, making it possible for HER2 to have an indirect inhibitory role on NOXA via TP53 (40). In addition, we have previously identified that entinostat can sensitize trastuzumab/lapatinib–resistant HER2-positive cells to treatment by induction of apoptosis via FOXO3-mediated Bim1 expression (11). Therefore, future studies into the potential role of HER2 positivity in relation to NOXA, as well as a potential rationale for an entinostat–trastuzumab–pimasertib triple combination therapy for instance, needs to be further explored as a possible therapeutic approach in HER2-positive breast cancer.

Remaining unclear are the specific reasons why select IBC and TNBC cell lines have increased NOXA mRNA expression, and *NOXA* promoter acetylation, in response to entinostat. Here we noted a tendency for *TP53*- and *BRCA1*-mutant cell lines to be unresponsive to treatment. *BRCA1* is a coactivator of *TP53* which subsequently induces apoptosis via NOXA,

Figure 6.

Entinostat and pimasertib combination treatment inhibits colony formation *in vitro* and tumor growth *in vivo* by NOXA-mediated apoptosis and decreased expression of MCL1. SUM190PT and SUM149PT cell lines were treated with entinostat (0.01 and 0.05 μmol/L, respectively) and/or pimasertib (0.01 and 0.05 μmol/L, respectively) and allowed to grow in an anchorage-independent environment for 2–3 weeks; clonal growth was measured at the treatment endpoint by colony formation (**A**). Data were pooled from three independent experiments and presented as mean ± SEM. Tumor volume measurements for SUM190PT and SUM149PT tumor xenograft-bearing mice ($n = 12$/group and 10/group, respectively) treated via oral gavage daily for up to 2 months with vehicle, entinostat (20 or 5 mg/kg), and/or pimasertib (30 or 0.5 mg/kg) (**B**). **C,** Immunohistochemistry (IHC) staining from SUM190PT and SUM149PT tumor xenografts treated with vehicle or the indicated drugs. Paraformaldehyde-fixed paraffin sections were incubated with anti-Ki-67 antibody, and TUNEL staining was performed. Representative images of 5 IHC staining experiments are illustrated. Magnification, 20×. The images were converted by ImageJ software to accomplish quantification of Ki-67 and TUNEL expression. Quantification of IHC staining is represented as mean ± SEM. **D** and **E,** Protein expression (represented as mean ± SEM) relative to loading control after immunoblotting analysis of NOXA, MCL1, and cleaved caspase-9 expression in protein lysates of five representative tumor samples from each treatment group of mice bearing SUM190PT or SUM149PT tumors. Tubulin expression was used as a protein loading control. Pixel density of protein bands was quantified for each condition using ImageJ software. *, $P < 0.05$; **, $P < 0.001$; ***, $P < 0.0001$.

suggesting a possible escape mechanism when *BRCA1* and *TP53* are mutated (14). In addition, we cannot rule out as possible contributing factors the potential differences in the intracellular metabolism of entinostat across cell lines, as well as other possible mechanism by which entinostat could be modulating *NOXA* gene expression. Future investigation into the role of *TP53* and *BRCA1* mutation status and entinostat intracellular metabolism in association with NOXA expression and treatment response would be of importance, potentially enabling additional criteria for patient selection.

Inhibition of proapoptotic NOXA through siRNA, as well as vector-induced expression of antiapoptotic MCL1, significantly induced resistance of SUM190PT and SUM149PT cells to entinostat and pimasertib separately, as well as to combination treatment, when compared with control transfections. Our findings confirmed the important role NOXA plays in sensitivity of TNBC and IBC cell lines to combination treatment, in that transient transfection of a NOXA-expressing vector reduced MCL1 protein levels, as well as sensitized the cells in combination with pimasertib. Further experiments should be done to provide more evidence supporting the direct role of NOXA and MCL1 driving combination treatment sensitivity, such as by developing NOXA and MCL1 protein inducible expression/suppression models, as well as constructs with mutated functional domains to determine their individual roles affecting combination treatment synergy.

IBC and TNBC remain diseases without an effective targeted therapy that can significantly affect patients' morbidity and/or survival. Our study provides preclinical evidence for the translational potential of a combined entinostat and pimasertib therapy for patients with the most aggressive molecular and clinical diagnoses of breast cancer, TNBC and IBC, especially for those with tumors expressing high levels of MCL1 and p-ERK, or increased levels following initial entinostat treatment. Although p-ERK has been reported to be a biomarker of poor prognosis in breast cancer (41), a potential challenge for the clinical application of our therapeutic strategy is that there are no treatment-predictive biomarkers established for the selection of patients who could benefit from MCL1-inhibition treatment. With the goal of discovering such a biomarker, a chemical genomic study identified that tumors with low expression of BCL-xL, an antiapoptotic BCL2 family member, were associated with sensitivity of breast and non–small cell lung cancer tumors *in vivo* to compounds that inhibit MCL1, representing a potential strategy that may be established in the clinic for the selection of patients who could benefit from MCL1 inhibition treatments (42). More importantly, the genomic and proteomic analyses performed in our current study are translatable to the clinical trial setting, allowing the study of baseline and treatment-induced MCL1 and NOXA expression levels in patient tumors. As supported by the results of our *in vivo* studies, the inclusion of MCL1 and NOXA expression measurement could provide robust predictive biomarkers of treatment response to entinostat and pimasertib combination therapy.

Besides breast cancer (43), overexpression of MCL1 has been associated with survival pathways, resistance, and poor prognosis in multiple cancers, such as melanoma (20), small-cell lung cancer (44), colorectal cancer (45), oral cancers (46), endometrial cancer (47), as well as multiple hematologic malignancies (21, 48). Therefore, our combination treatment may be effective in other cancers increasing the impact of this study. However, further validation in clinically relevant models for each disease is needed. Others have reported data supporting the potential for the combination treatment of MCL1 inhibitors and inducers of NOXA, providing further evidence of the likely applicability of our combination treatment (49, 50). Furthermore, we observed sensitivity of IBC and TNBC cells to entinostat and pimasertib treatment within clinically relevant concentrations, providing a preclinical rationale for translation into a clinically appropriate dose.

In summary, we demonstrate the efficacy of combined HDAC inhibitor entinostat and MEK inhibitor pimasertib treatment blocking the progression of preclinical models of TNBC and IBC. Effective therapy was significantly associated to the induction of tumor apoptosis regulated by NOXA-mediated MCL1 degradation. Collectively, our results provide a strong rationale for clinical drug and predictive biomarker studies for this combination therapy in IBC and TNBC.

Disclosure of Potential Conflicts of Interest

P. Ordentlich holds ownership interest (including patents) in Syndax Pharmaceuticals. No potential conflicts of interest were disclosed by the other authors.

Authors' Contributions

Conception and design: A.M. Torres-Adorno, J. Lee, N.T. Ueno
Development of methodology: A.M. Torres-Adorno, J. Lee, N.T. Ueno
Acquisition of data (provided animals, acquired and managed patients, provided facilities, etc.): A.M. Torres-Adorno, J. Lee, T. Kogawa
Analysis and interpretation of data (e.g., statistical analysis, biostatistics, computational analysis): A.M. Torres-Adorno, J. Lee, T. Kogawa, D. Tripathy, N.T. Ueno
Writing, review, and/or revision of the manuscript: A.M. Torres-Adorno, J. Lee, T. Kogawa, P. Ordentlich, D. Tripathy, B. Lim, N.T. Ueno
Administrative, technical, or material support (i.e., reporting or organizing data, constructing databases): A.M. Torres-Adorno, T. Kogawa, N.T. Ueno
Study supervision: J. Lee, N.T. Ueno
Other (project coordinator): A.M. Torres-Adorno

Acknowledgments

We thank Sunita Patterson and Christopher Graber of the Department of Scientific Publications and Dr. Bedrich Eckhardt of the Department of Breast Medical Oncology at the MD Anderson Cancer Center for their expert editorial assistance. Entinostat was provided by Syndax Pharmaceuticals Inc. Pimasertib was provided by EMD Serono, Inc., an affiliate of Merck KGaA, Germany.

Grant Support

This work was supported by the Morgan Welch Inflammatory Breast Cancer Research Program, the State of Texas Rare and Aggressive Breast Cancer Research Program, the NIH/National Cancer Institute (CA123318; to N.T. Ueno), MD Anderson's Cancer Center Support Grant (R01CA123318 and P30CA016672, used the Characterized Cell Line Core Facility, and Flow Cytometry and Cellular Imaging Facility), Syndax Pharmaceuticals, Inc., and EMD Serono, Inc.

The costs of publication of this article were defrayed in part by the payment of page charges. This article must therefore be hereby marked *advertisement* in accordance with 18 U.S.C. Section 1734 solely to indicate this fact.

Received October 18, 2016; revised February 26, 2017; accepted April 27, 2017; published OnlineFirst May 2, 2017.

References

1. Dawood S, Ueno NT, Valero V, Woodward WA, Buchholz TA, Hortobagyi GN, et al. Differences in survival among women with stage III inflammatory and noninflammatory locally advanced breast cancer appear early: a large population-based study. Cancer 2011;117:1819–26.
2. Criscitiello C, Azim HA Jr, Schouten PC, Linn SC, Sotiriou C. Understanding the biology of triple-negative breast cancer. Ann Oncol 2012;23Suppl 6: vi13–8.
3. Matsumoto H, Koo SL, Dent R, Tan PH, Iqbal J. Role of inflammatory infiltrates in triple negative breast cancer. J Clin Pathol 2015;68:506–10.
4. Bae SY, Kim S, Lee JH, Lee HC, Lee SK, Kil WH, et al. Poor prognosis of single hormone receptor- positive breast cancer: similar outcome as triple-negative breast cancer. BMC Cancer 2015;15:138.
5. Li J, Gonzalez-Angulo AM, Allen PK, Yu TK, Woodward WA, Ueno NT, et al. Triple-negative subtype predicts poor overall survival and high locoregional relapse in inflammatory breast cancer. Oncologist 2011;16: 1675–83.
6. Chaher N, Arias-Pulido H, Terki N, Qualls C, Bouzid K, Verschraegen C, et al. Molecular and epidemiological characteristics of inflammatory breast cancer in Algerian patients. Breast Cancer Res Treat 2012;131:437–44.
7. Zell JA, Tsang WY, Taylor TH, Mehta RS, Anton-Culver H. Prognostic impact of human epidermal growth factor-like receptor 2 and hormone receptor status in inflammatory breast cancer (IBC): analysis of 2,014 IBC patient cases from the California Cancer Registry. Breast Cancer Res 2009;11:R9.
8. Mottamal M, Zheng S, Huang TL, Wang G. Histone deacetylase inhibitors in clinical studies as templates for new anticancer agents. Molecules 2015;20:3898–941.
9. Saito A, Yamashita T, Mariko Y, Nosaka Y, Tsuchiya K, Ando T, et al. A synthetic inhibitor of histone deacetylase, MS-27-275, with marked in vivo antitumor activity against human tumors. Proc Natl Acad Sci U S A 1999;96:4592–7.
10. Yardley DA, Ismail-Khan RR, Melichar B, Lichinitser M, Munster PN, Klein PM, et al. Randomized phase II, double-blind, placebo-controlled study of exemestane with or without entinostat in postmenopausal women with locally recurrent or metastatic estrogen receptor-positive breast cancer progressing on treatment with a nonsteroidal aromatase inhibitor. J Clin Oncol 2013;31:2128–35.
11. Lee J, Bartholomeusz C, Mansour O, Humphries J, Hortobagyi GN, Ordentlich P, et al. A class I histone deacetylase inhibitor, entinostat, enhances lapatinib efficacy in HER2-overexpressing breast cancer cells through FOXO3-mediated Bim1 expression. Breast Cancer Res Treat 2014;146:259–72.
12. Danial NN. BCL-2 family proteins: critical checkpoints of apoptotic cell death. Clin Cancer Res 2007;13:7254–63.
13. Fritsche P, Seidler B, Schuler S, Schnieke A, Gottlicher M, Schmid RM, et al. HDAC2 mediates therapeutic resistance of pancreatic cancer cells via the BH3-only protein NOXA. Gut 2009;58:1399–409.
14. Inoue S, Riley J, Gant TW, Dyer MJ, Cohen GM. Apoptosis induced by histone deacetylase inhibitors in leukemic cells is mediated by Bim and Noxa. Leukemia 2007;21:1773–82.
15. Goodwin CM, Rossanese OW, Olejniczak ET, Fesik SW. Myeloid cell leukemia-1 is an important apoptotic survival factor in triple-negative breast cancer. Cell Death Differ 2015;22:2098–106.
16. Mei Y, Du W, Yang Y, Wu M. Puma(*)Mcl-1 interaction is not sufficient to prevent rapid degradation of Mcl-1. Oncogene 2005;24:7224–37.
17. Czabotar PE, Lee EF, van Delft MF, Day CL, Smith BJ, Huang DC, et al. Structural insights into the degradation of Mcl-1 induced by BH3 domains. Proc Natl Acad Sci U S A 2007;104:6217–22.
18. Ploner C, Kofler R, Villunger A. Noxa: at the tip of the balance between life and death. Oncogene 2008;27Suppl 1:S84–92.
19. Mitchell C, Yacoub A, Hossein H, Martin AP, Bareford MD, Eulitt P, et al. Inhibition of MCL-1 in breast cancer cells promotes cell death in vitro and in vivo. Cancer Biol Ther 2010;10:903–17.
20. Chetoui N, Sylla K, Gagnon-Houde JV, Alcaide-Loridan C, Charron D, Al-Daccak R, et al. Down-regulation of mcl-1 by small interfering RNA sensitizes resistant melanoma cells to fas-mediated apoptosis. Mol Cancer Res 2008;6:42–52.
21. Konopleva M, Milella M, Ruvolo P, Watts JC, Ricciardi MR, Korchin B, et al. MEK inhibition enhances ABT-737-induced leukemia cell apoptosis via prevention of ERK-activated MCL-1 induction and modulation of MCL-1/BIM complex. Leukemia 2012;26:778–87.
22. Bartholomeusz C, Gonzalez-Angulo AM, Liu P, Hayashi N, Lluch A, Ferrer-Lozano J, et al. High ERK protein expression levels correlate with shorter survival in triple-negative breast cancer patients. Oncologist 2012;17:766–74.
23. Adjei AA, Cohen RB, Franklin W, Morris C, Wilson D, Molina JR, et al. Phase I pharmacokinetic and pharmacodynamic study of the oral, small-molecule mitogen-activated protein kinase kinase 1/2 inhibitor AZD6244 (ARRY-142886) in patients with advanced cancers. J Clin Oncol 2008; 26:2139–46.
24. Bartholomeusz C, Oishi T, Saso H, Akar U, Liu P, Kondo K, et al. MEK1/2 inhibitor selumetinib (AZD6244) inhibits growth of ovarian clear cell carcinoma in a PEA-15-dependent manner in a mouse xenograft model. Mol Cancer Ther 2012;11:360–9.
25. Kim K, Kong SY, Fulciniti M, Li X, Song W, Nahar S, et al. Blockade of the MEK/ERK signalling cascade by AS703026, a novel selective MEK1/2 inhibitor, induces pleiotropic anti-myeloma activity in vitro and in vivo. Br J Haematol 2010;149:537–49.
26. Awada A, Delord JP, Houede N, Lebbe C, Lesimple T, Schellens JHM, et al. Safety and recommended phase II dose (RP2D) of the selective oral MEK1/2 inhibitor pimasertib (MSC1936369B/AS703026): Results of a phase I trial. European J Cancer 2012;48:18586.
27. Catalanotti F, Solit DB, Pulitzer MP, Berger MF, Scott SN, Iyriboz T, et al. Phase II trial of MEK inhibitor selumetinib (AZD6244, ARRY-142886) in patients with BRAFV600E/K-mutated melanoma. Clin Cancer Res 2013; 19:2257–64.
28. Farley J, Brady WE, Vathipadiekal V, Lankes HA, Coleman R, Morgan MA, et al. Selumetinib in women with recurrent low-grade serous carcinoma of the ovary or peritoneum: an open-label, single-arm, phase 2 study. Lancet Oncol 2013;14:134–40.
29. Bartholomeusz C, Xie X, Pitner MK, Kondo K, Dadbin A, Lee J, et al. MEK inhibitor selumetinib (AZD6244; ARRY-142886) prevents lung metastasis in a triple-negative breast cancer xenograft model. Mol Cancer Ther 2015; 14:2773–81.
30. Van Laere SJ, Ueno NT, Finetti P, Vermeulen P, Lucci A, Robertson FM, et al. Uncovering the molecular secrets of inflammatory breast cancer biology: an integrated analysis of three distinct affymetrix gene expression datasets. Clin Cancer Res 2013;19:4685–96.
31. Bertucci F, Ueno NT, Finetti P, Vermeulen P, Lucci A, Robertson FM, et al. Gene expression profiles of inflammatory breast cancer: correlation with response to neoadjuvant chemotherapy and metastasis-free survival. Ann Oncol 2014;25:358–65.
32. Klopp AH, Lacerda L, Gupta A, Debeb BG, Solley T, Li L, et al. Mesenchymal stem cells promote mammosphere formation and decrease E-cadherin in normal and malignant breast cells. PLoS One 2010;5:e12180.
33. Kurebayashi J, Otsuki T, Tang CK, Kurosumi M, Yamamoto S, Tanaka K, et al. Isolation and characterization of a new human breast cancer cell line, KPL-4, expressing the Erb B family receptors and interleukin-6. Br J Cancer 1999;79:707–17.
34. Lehmann BD, Bauer JA, Chen X, Sanders ME, Chakravarthy AB, Shyr Y, et al. Identification of human triple-negative breast cancer subtypes and preclinical models for selection of targeted therapies. J Clin Invest 2011;121: 2750–67.
35. Zhou L, Ruvolo VR, McQueen T, Chen W, Samudio IJ, Conneely O, et al. HDAC inhibition by SNDX-275 (Entinostat) restores expression of silenced leukemia-associated transcription factors Nur77 and Nor1 and of key pro-apoptotic proteins in AML. Leukemia 2013;27:1358–68.
36. Baou M, Kohlhaas SL, Butterworth M, Vogler M, Dinsdale D, Walewska R, et al. Role of NOXA and its ubiquitination in proteasome inhibitor-induced apoptosis in chronic lymphocytic leukemia cells. Haematologica 2010;95:1510–8.
37. Singh TR, Shankar S, Srivastava RK. HDAC inhibitors enhance the apoptosis-inducing potential of TRAIL in breast carcinoma. Oncogene 2005;24:4609–23.
38. Gomez-Bougie P, Menoret E, Juin P, Dousset C, Pellat-Deceunynck C, Amiot M. Noxa controls Mule-dependent Mcl-1 ubiquitination through the regulation of the Mcl-1/USP9X interaction. Biochem Biophys Res Commun 2011;413:460–4.
39. Rosato RR, Almenara JA, Grant S. The histone deacetylase inhibitor MS-275 promotes differentiation or apoptosis in human leukemia cells through a process regulated by generation of reactive oxygen species and induction of p21CIP1/WAF1 1. Cancer Res 2003;63:3637–45.

40. Carpenter RL, Lo HW. Regulation of apoptosis by HER2 in breast cancer. J Carcinog Mutagen 2013;S7:003.
41. Milde-Langosch K, Bamberger AM, Rieck G, Grund D, Hemminger G, Muller V, et al. Expression and prognostic relevance of activated extracellular-regulated kinases (ERK1/2) in breast cancer. Br J Cancer 2005;92:2206–15.
42. Wei G, Margolin AA, Haery L, Brown E, Cucolo L, Julian B, et al. Chemical genomics identifies small-molecule MCL1 repressors and BCL-xL as a predictor of MCL1 dependency. Cancer Cell 2012;21:547–62.
43. Balko JM, Giltnane JM, Wang K, Schwarz LJ, Young CD, Cook RS, et al. Molecular profiling of the residual disease of triple-negative breast cancers after neoadjuvant chemotherapy identifies actionable therapeutic targets. Cancer Discov 2014;4:232–45.
44. Hauck P, Chao BH, Litz J, Krystal GW. Alterations in the Noxa/Mcl-1 axis determine sensitivity of small cell lung cancer to the BH3 mimetic ABT-737. Mol Cancer Ther 2009;8:883–92.
45. Mattoo AR, Zhang J, Espinoza LA, Jessup JM. Inhibition of NANOG/NANOGP8 downregulates MCL-1 in colorectal cancer cells and enhances the therapeutic efficacy of BH3 mimetics. Clin Cancer Res 2014;20:5446–55.
46. Palve V, Mallick S, Ghaisas G, Kannan S, Teni T. Overexpression of Mcl-1L splice variant is associated with poor prognosis and chemoresistance in oral cancers. PLoS One 2014;9:e111927.
47. Konno Y, Dong P, Xiong Y, Suzuki F, Lu J, Cai M, et al. MicroRNA-101 targets EZH2, MCL-1 and FOS to suppress proliferation, invasion and stem cell-like phenotype of aggressive endometrial cancer cells. Oncotarget 2014;5:6049–62.
48. Hermanson DL, Das SG, Li Y, Xing C. Overexpression of Mcl-1 confers multidrug resistance, whereas topoisomerase IIbeta downregulation introduces mitoxantrone-specific drug resistance in acute myeloid leukemia. Mol Pharmacol 2013;84:236–43.
49. Geserick P, Wang J, Feoktistova M, Leverkus M. The ratio of Mcl-1 and Noxa determines ABT737 resistance in squamous cell carcinoma of the skin. Cell Death Dis 2014;5:e1412.
50. Yan J, Zhong N, Liu G, Chen K, Liu X, Su L, et al. Usp9x- and Noxa-mediated Mcl-1 downregulation contributes to pemetrexed-induced apoptosis in human non-small-cell lung cancer cells. Cell Death Dis 2014;5:e1316.